International Journal of Heat and Technology
Vol. 41, No. 6, December, 2023, pp. 1639-1644
Journal homepage: http://iieta.org/journals/ijht

Solidification and Conformation of Ionic Liquid 1-Ethyl-3-Methylimidazolium Trifluoroacetate under High Pressure

Haining Li[1,2,3*], Yu Lin[1]

[1] Henan Key Laboratory of Magnetoelectric Information Functional Materials, School of Electronics and Information, Zhengzhou University of Light Industry, Zhengzhou 450002, China
[2] School of Physics and Electronics, Henan University, Kaifeng 475004, China
[3] Zhengzhou Vcom Science and Technology Co., Ltd, Zhengzhou 450002, China

Corresponding Author Email: lihaining@zzuli.edu.cn

https://doi.org/10.18280/ijht.410627

Received: 15 June 2023
Revised: 23 September 2023
Accepted: 16 October 2023
Available online: 31 December 2023

Keywords:
imidazolium-based ionic liquids, high pressure, Raman spectra, phase transition, conformation

ABSTRACT

The structural dynamics and phase behavior of 1-ethyl-3-methylimidazolium trifluoroacetate ([Emim][CF_3AcO]) under elevated pressure conditions were meticulously examined. Utilizing a diamond-anvil cell (DAC) in conjunction with Raman spectroscopy and synchrotron radiation X-ray diffraction, investigations were conducted at ambient temperature. Synchrotron radiation X-ray diffraction spectra revealed the absence of crystallization in the samples at pressures up to 5 GPa. A detailed analysis of the Raman spectra elucidated the relationships between Raman shift and full width at half maxima (FWHM) of characteristic Raman peaks as a function of pressure. A notable discontinuity was observed around 2.8 GPa, suggestive of a potential phase transition at this threshold. The hydrostatic properties of [Emim][CF_3AcO] were further elucidated through analysis based on the ruby fluorescence peak under high-pressure conditions. These findings indicate a pressure-induced transition of [Emim][CF_3AcO] at approximately 2.8 GPa, transitioning from a liquid state to a superpressurized glass. In addition, the conformational equilibrium of [Emim][CF_3AcO] under such high-pressure environments was meticulously analyzed. The study revealed the coexistence of two conformers, namely planar and nonplanar, under high-pressure conditions. It was observed that the population of planar conformers escalates with increasing pressure, attributable to their reduced conformational volume. This research provides novel insights into the high-pressure behavior of imidazolium-based ILs, contributing significantly to the understanding of their phase transitions and conformational dynamics under extreme conditions.

1. INTRODUCTION

ILs, organic salts composed entirely of ions and liquid at or near room temperature, have emerged as a focal point in scientific research due to their unique properties. Characterized by non-volatility, low melting points, and a broad electrochemical window, these substances offer promising applications in diverse fields such as chemical engineering, electrochemistry, and biotechnology. Additionally, ILs are recognized as environmentally friendly and designable solvents, garnering considerable attention within the scientific community [1-5].

The study of materials invariably involves three critical physical parameters: pressure, temperature, and composition. Pressure, in particular, serves as a pivotal factor in altering interatomic or intermolecular distances, thus inducing high-pressure phase transitions and unveiling novel structures and properties. With advancements in high-pressure techniques, this parameter has gained prominence as an experimental approach to probe the physical and chemical characteristics of materials. While the majority of ILs research has concentrated on their properties under ambient conditions, recent years have witnessed a growing interest in understanding these substances under high-pressure scenarios. Pioneering studies by Yoshimura et al. have shed light on the phase behavior of 1-ethyl-3-methylimidazolium tetrafluoroborate ([EMIM][BF_4]), observing a glass transition around 2.8 GPa without crystallization up to 7 GPa. Interestingly, during decompression, crystallization occurred at approximately 2.0 GPa and 1.0 GPa [6]. Furthermore, investigations into the stability of 1-butyl-3-methylimidazolium iodide ([Bmim][I]) under high pressure at room temperature revealed the formation of a glassy state at 1.3 GPa, with partial crystallization at 16.7 GPa [7].

The structural dynamics and phase transitions of ILs with trifluoromethanesulfonate anions have been extensively examined by Ribeiro et al., with a particular focus on the conformational equilibria of cations and the determination of glass transition pressures [8]. Furthermore, systematic studies on the structures and phase behaviors of 1-alkyl-3-methylimidazolium hexafluorophosphate under high-pressure conditions have been conducted [9-14]. These investigations are pivotal in enhancing the comprehension of ILs' structural and phase characteristics under extreme conditions, thereby contributing significantly to the elucidation of their phase transition mechanisms in high-pressure environments.

Imidazole-based ILs, comprising 1-alkyl-3-methylimidazole cations and various anions, stand out for their ease of synthesis and structural versatility, making them among the most extensively researched ILs. Probing the structural and property dynamics of these ILs under high pressure is crucial for a deeper understanding of their unique characteristics and lays the foundation for their application in extreme environments. In this study, Raman spectroscopy and synchrotron radiation X-ray diffraction have been employed to investigate the structure and phase transitions of [Emim][CF_3AcO] under high pressure. Additionally, a detailed analysis of the conformational equilibrium of cations under these conditions is presented. This research not only augments the fundamental knowledge base of ILs but also broadens the scope of their application in extreme conditions.

2. EXPERIMENT

The IL [Emim][CF_3AcO] was procured from the Lanzhou Institute of Chemical Physics, Chinese Academy of Sciences. Its purity was ascertained to be in excess of 99.5%. Prior to spectroscopic analysis, the sample underwent a drying process under vacuum at 333 K for a minimum duration of three days, aiming to minimize the presence of moisture and volatile compounds. The molecular weight of the sample was determined to be 224.18 g/mol. Characterized by a melting point of 223 K, [Emim][CF_3AcO] remains in a liquid state under standard room temperature and pressure conditions. The molecular structure of [Emim][CF_3AcO] is illustrated in Figure 1. It features a cation comprising an imidazole ring, substituted at the 1 and 3 positions with ethyl and methyl groups, respectively. The accompanying anion in this IL is trifluoroacetate.

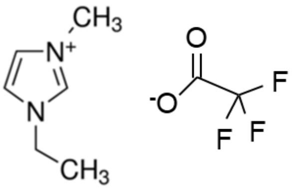

Figure 1. Schematic representation of the molecular structure of [Emim][CF_3AcO]

Raman spectroscopic measurements were conducted utilizing a Renishaw inVia Raman microscope (Renishaw, UK), equipped with a 532 nm semiconductor laser with a power output of 50 mW for excitation. High pressure was generated using a DAC, featuring a 350 μm diameter diamond anvil. The gasket, composed of T301 stainless steel, underwent preindentation to a thickness of 100 μm and subsequent laser drilling to create a sample cavity with a diameter of approximately 150 μm. Experiments were performed at an ambient temperature of 298 K. The liquid [Emim][CF_3AcO] was carefully placed into the sample cavity at the center of the gasket, accompanied by a ruby particle serving as a pressure gauge. The pressure exerted on the sample was deduced from the frequency shift of the ruby R_1 line [15]. To ensure equilibrium conditions, each sample was stabilized for a minimum of 5 minutes before Raman spectra collection.

In-situ high-pressure X-ray diffraction experiments were carried out at the X17C station of the National Synchrotron Radiation Source at Brookhaven National Laboratory, USA. The incident X-ray beam, with a wavelength of 0.4066 Å, was directed onto the sample, having a beam size of approximately 26.6×24 μm^2. Diffraction patterns were captured using a CCD detector and subsequently processed using Fit2D code software for pattern integration [16].

3. RESULTS AND DISCUSSION

The Raman spectroscopic analysis of [Emim][CF_3AcO] under varying pressure levels at room temperature (298K) is depicted in Figure 2. Building upon existing studies [17-19], the observed Raman peaks at 596, 701, 718, 825, and 1022 cm^{-1} are respectively attributed to the in-plane symmetric bending vibration of the imidazole ring, in-plane asymmetric bending vibration of the imidazole ring, symmetric deformation vibration of CF_3 in the anion, C-C stretching vibration in the anion, and in-plane symmetric stretching vibration of the imidazole ring in the cation. Moreover, the Raman spectral ranges of 2800-3050 cm^{-1} and 3050-3200 cm^{-1} are recognized as the C-H stretching vibrations of the alkyl chain and imidazole ring in the cations, respectively.

A notable observation was that with pressure escalation up to approximately 5 GPa, the Raman spectra of [Emim][CF_3AcO] exhibited no emergence of new peaks, although a decline in spectral resolution was recorded. It was observed that the Raman characteristic peaks of the sample underwent a blue shift as pressure increased. This shift is attributed to the compression-induced reduction in interatomic distances within the molecules, leading to the contraction of the imidazole ring and a consequent decrease in the lengths of hydrocarbon, carbon-nitrogen, and carbon-carbon bonds. The diminution of bond lengths correlated with an elevation in bond energy, manifesting as a blue shift in the Raman spectra.

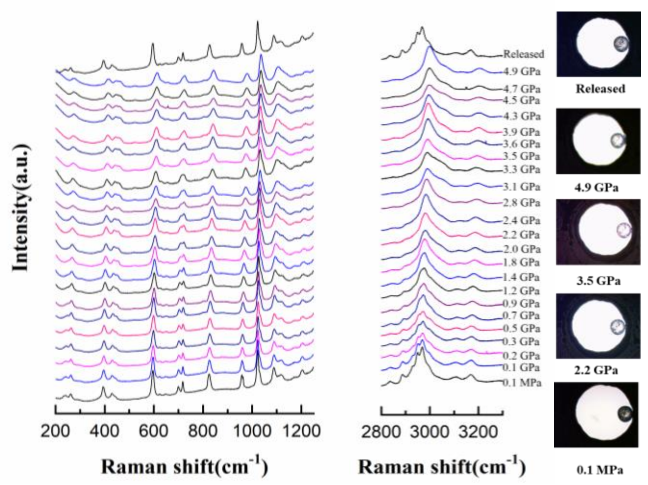

Figure 2. Raman spectra of IL [Emim][CF_3AcO] under high pressure (298 K)

The Raman peaks within the spectral range of 2800-3050 cm^{-1}, associated with the stretching vibrations of the alkyl chain C-H in the cation $[Emim]^+$, presented a degree of complexity in their specific identification. However, an increase in pressure resulted in the convergence of these peaks into a singular peak. Furthermore, a comparison between the Raman spectra of the C-H stretching vibrations in the alkyl chain and the imidazole ring of the $[Emim]^+$ under compression revealed a more pronounced alteration in the former. This indicates that the structural adjustments in the alkyl chain were more significant than those in the imidazole ring under high-pressure conditions, likely due to the inherent flexibility of the side-chain alkyl group.

Figure 2 further presents the Raman spectra of $[Emim][CF_3AcO]$ following pressure release, alongside micrographs depicting the sample cavity under various pressures. It was observed that no discernible crystallization occurred within the sample cavity throughout the experimental procedure. Moreover, upon depressurization to ambient pressure, the Raman spectra of the sample exhibited recovery, closely resembling the spectra obtained under ambient conditions. This consistency suggests that $[Emim][CF_3AcO]$ maintained its chemical stability and did not undergo crystallization even after being subjected to pressures of approximately 5 GPa.

For an enhanced understanding of the structural dynamics of $[Emim][CF_3AcO]$ under high pressure, the peak positions of the Raman spectra were meticulously fitted and analyzed as a function of pressure, as depicted in Figure 3(a). An inflection point in the slope of the Raman shifts as a function of pressure was observed at approximately 2.8 GPa. This inflection suggests the possibility of a phase transition occurring near 2.8 GPa. Additionally, Figure 3(b) illustrates the FWHM of the Raman peaks under high pressure. A discontinuity in the FWHM at 2.8 GPa further corroborates the hypothesis of a phase transition in $[Emim][CF_3AcO]$ around this pressure threshold.

To further elucidate the phase state of $[Emim][CF_3AcO]$ beyond the 2.8 GPa threshold, synchrotron radiation X-ray diffraction analysis was employed, as illustrated in Figure 4. The X-ray diffraction spectra of $[Emim][CF_3AcO]$ under high pressure demonstrated minimal changes up to 5 GPa, with the diffraction pattern predominantly displaying a halo pattern. The absence of sharp Bragg peaks in the high-pressure diffraction pattern indicates that $[Emim][CF_3AcO]$ did not crystallize and remained in a liquid or amorphous state up to 5 GPa.

Considering that $[Emim][CF_3AcO]$ is in a liquid state at atmospheric pressure, a transition to a solid state under high pressure would alter the sample chamber from a hydrostatic to a non-hydrostatic environment. Typically, the hydrostaticity of the sample cavity can be determined by two methods: 1) Variation in the FWHM of the ruby R_1 line as a function of pressure [20], and 2) The differential between the peak positions of ruby R_1 and R_2 lines (R1-R2) as a function of pressure [21]. The pressure point at which an increase in these parameters is observed is identified as the glass transition pressure (P_g). Accordingly, Figure 5 analyzes the deviation in FWHM of the ruby R_1 line under high pressure from its ambient pressure value, as well as the R_1-R_2 differential under varying pressures. In Figure 5(a), below 2.8 GPa, a slight decrease in the FWHM difference value of the ruby R_1 line was noted. Beyond 2.8 GPa, this difference value continued to increase, displaying an inflection point around 2.8 GPa. This observation suggests that the IL $[Emim][CF_3AcO]$ likely underwent a glass transition near 2.8 GPa.

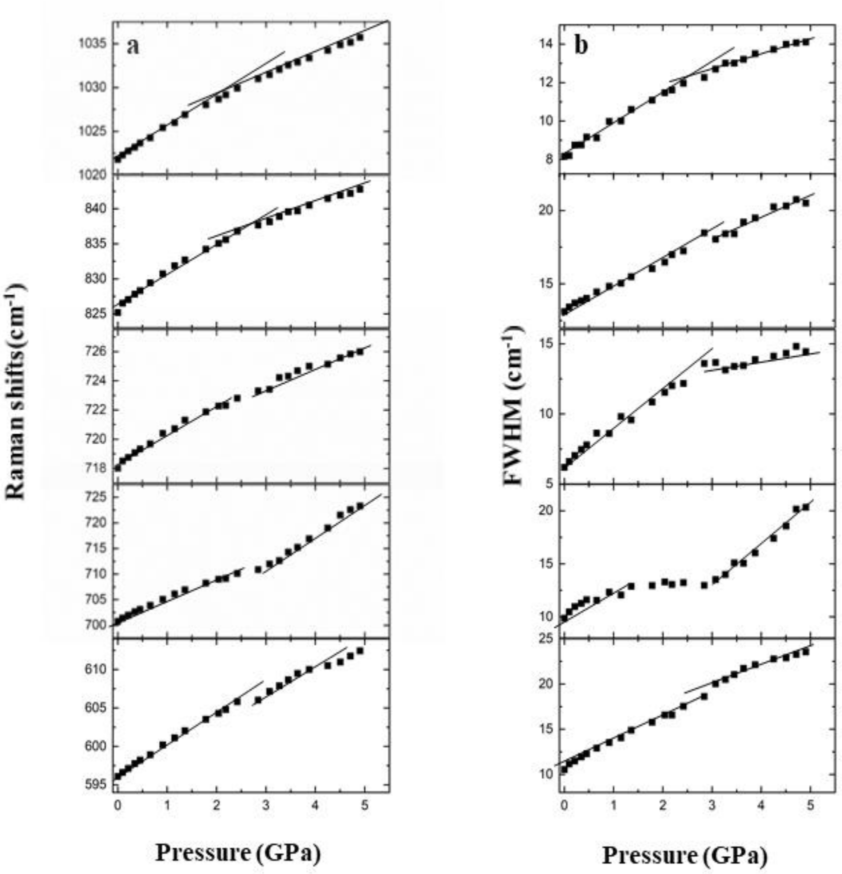

Figure 3. (a) Raman shifts and (b) FWHM of $[Emim][CF_3AcO]$ under high pressure

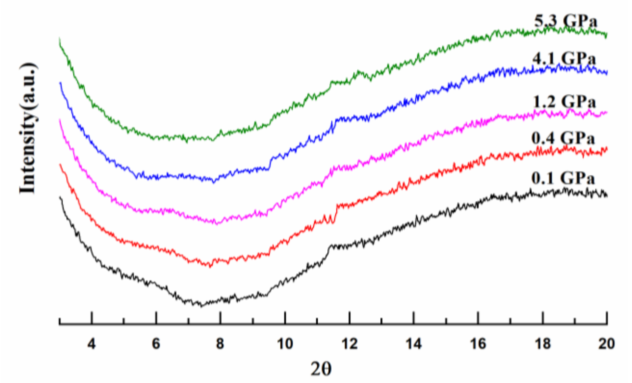

Figure 4. Synchrotron radiation X-ray diffraction spectrum of [Emim][CF_3AcO] under high pressure

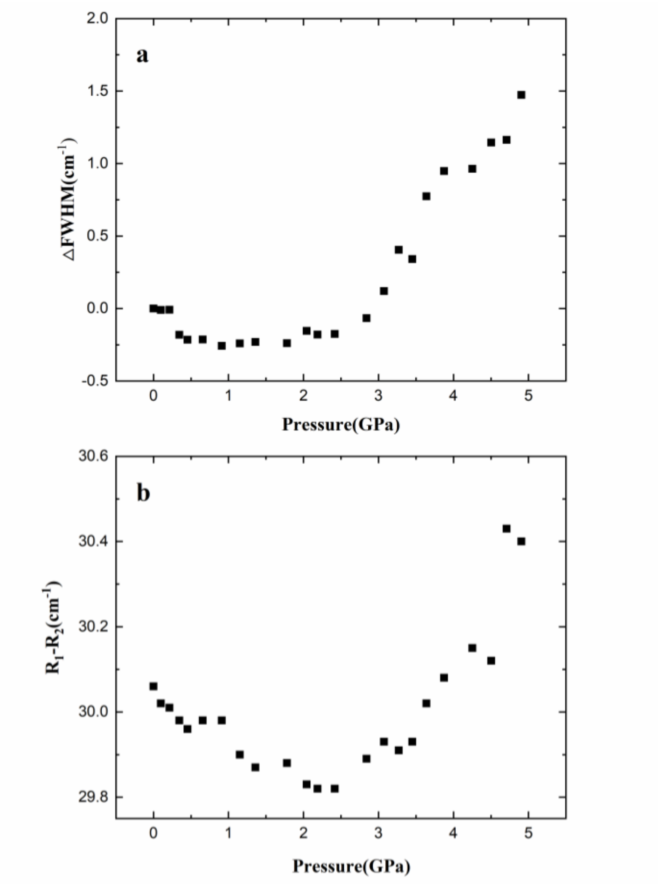

Figure 5. (a) Difference in FWHM of the ruby R_1 line under high pressure and compared to ambient pressure, and (b) pressure dependence of R_1–R_2 splitting for [Emim][CF_3AcO]

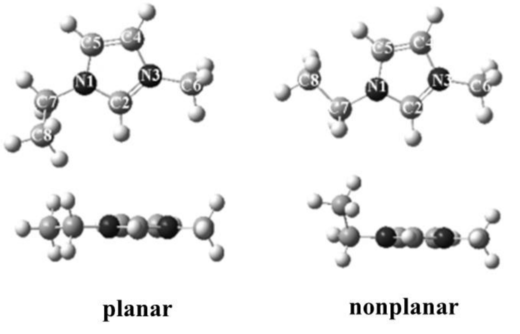

Figure 6. Schematic diagram of planar and non-planar conformational structures of the cation [Emim]$^+$

Furthermore, the uniaxial stress exerted on ruby is known to influence the disparity in peak positions between the ruby R_1 and R_2 lines [21], thus establishing the R_1-R_2 difference as an indicator of hydrostatic pressure. As depicted in Figure 5(b), a discontinuity in the R_1-R_2 difference was also observed at 2.8 GPa, lending additional support to the notion of a glass transition occurring around this pressure. Consequently, it is inferred that [Emim][CF_3AcO] transitions to a glassy state up to 5 GPa, with the glass transition pressure identified at 2.8 GPa.

In summary, the glass transition of [Emim][CF_3AcO] from a liquid to an amorphous state at approximately 2.8 GPa is corroborated through an integrated analysis encompassing Raman shifts, FWHM of Raman peaks, synchrotron radiation X-ray diffraction, broadening of the ruby R_1 line, and the R_1-R_2 difference under high pressure conditions.

The propensity of imidazole rings' alkyl chains to adopt various conformations complicates the regular ion packing necessary for crystallization, possibly accounting for the difficulty in crystallizing ILs and their tendency to solidify in an amorphous state. Therefore, investigating the conformational equilibrium under high pressure is crucial for a deeper understanding of the glass state under such conditions. With respect to the cations, two distinct conformers, planar and non-planar, exist, contingent on the rotation angle of the ethyl chain in [Emim]$^+$ [22]. These conformers are depicted in Figure 6. To further scrutinize the conformational changes under compression, the spectra ranging from 325 to 500 cm^{-1} at various pressures were analyzed, as shown in Figure 7(a), to study the cation conformations. The Raman peaks at 430 and 445 cm^{-1} are indicative of non-planar and planar conformers, respectively [22], while the peak at 392 cm^{-1} is attributed to the deformation vibration of CCO_2 [17]. At room temperature and ambient pressure, the presence of both planar and non-planar conformer Raman peaks signifies the coexistence of these two conformers in the liquid state of the sample.

The Raman peaks at 430 and 445 cm^{-1} were selected to represent the non-planar and planar conformations, respectively. The intensity fractions of planar conformers were calculated using the following equation:

$$f_{\text{planar}} = \frac{I_{\text{planar}}}{I_{\text{planar}} + I_{\text{nonplanar}}} \tag{1}$$

where, I_{planar} and $I_{nonplanar}$ denote the Raman peak areas of the planar conformers (445 cm^{-1}) and non-planar conformer (430 cm^{-1}), respectively. Figure 7(b) displays the intensity fractions of planar conformers of [Emim][CF_3AcO] under different pressures. An increase in the intensity fractions of planar conformers with rising pressure was observed, signifying that the population of planar conformers progressively augmented upon compression. This observation aligns with the increase in intensity fractions of planar conformers in [Emim][CF_3SO_3] under high pressure [23]. This trend could be attributed to the comparatively smaller volume of planar conformers relative to non-planar ones. Consequently, a transformation from non-planar to planar conformers occurred, resulting in an increased population of planar conformers under compression. Notably, the rate of increase in planar conformers decelerated beyond 2.8 GPa upon further compression. This could be due to the solidification of the sample above 2.8 GPa, where the degree of disorder and conformational equilibrium were effectively 'frozen' near the glass transition pressure. Additionally, an inflection point near 2.8 GPa was identified in the relationship between the intensity fractions of planar conformers and pressure, consistent with the glass transition pressure.

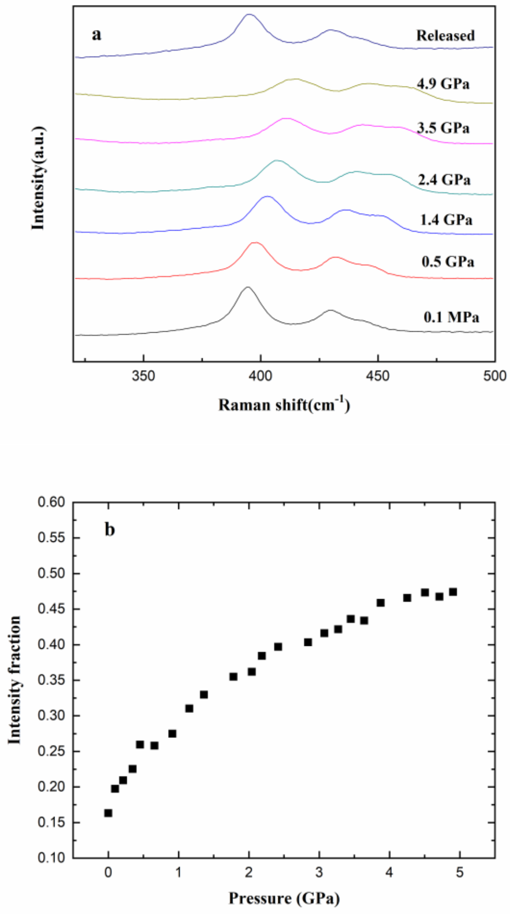

Figure 7. (a) Raman spectra of [Emim][CF_3AcO] conformers and (b) Intensity fractions of planar conformers under different pressures

4. CONCLUSION

This study has comprehensively examined the solidification and conformation of the IL [Emim][CF_3AcO] under compression. Utilizing a DAC apparatus, Raman spectroscopy and synchrotron radiation X-ray diffraction analyses were performed on [Emim][CF_3AcO] under high pressure. The findings indicate that [Emim][CF_3AcO] undergoes a phase transition around 2.8 GPa at room temperature. Analysis of the ruby fluorescence peak revealed that this transition is a glass transition, converting from a liquid to a glass state at 2.8 GPa. Additionally, the reversibility of the sample within a pressure range of up to 5 GPa was observed. The conformational equilibrium of the cation under high pressure was also investigated. Both planar and non-planar conformers were found to coexist, which may explain the amorphous solidification of [Emim][CF_3AcO] under high pressure. Notably, an increase in the population of planar conformers was observed, attributed to their smaller conformational volume. However, the trend in the intensity fractions of planar conformers demonstrated a deceleration above 2.8 GPa.

Future studies are poised to explore the structure and phase transitions of a broader range of ILs under high pressure. Such research endeavors could unveil the underlying principles of solidification in ILs and potentially broaden their application spectrum.

ACKNOWLEDGEMENTS

This work is supported by Post-doctoral research funding project of Henan Province (Grant No.: HN2022152).

REFERENCES

[1] Wasserscheid, P., Keim, W. (2000). Ionic Liquids-New "solutions" for transition metal catalysis. Angewandte Chemie International Edition, 39(21): 3772-3789. https://doi.org/10.1002/1521-3773(20001103)39:21%3C3772::AID-ANIE3772%3E3.0.CO;2-5

[2] Holbrey, J.D., Reichert, W.M., Swatloski, R.P., Broker, G.A., Pitner, W.R., Seddon, K.R., Rogers, R.D. (2002). Efficient, halide free synthesis of new, low cost ionic liquids: 1, 3-dialkylimidazolium salts containing methyl- and ethyl-sulfate anions. Green Chemistry, 4(5): 407-413. https://doi.org/10.1039/B204469B

[3] Armand, M., Endres, F., MacFarlane, D.R., Ohno, H., Scrosati, B. (2009). Ionic-liquid materials for the electrochemical challenges of the future. Nature Materials, 8(8): 621-629. https://doi.org/10.1038/nmat2448

[4] Han, X., Armstrong, D.W. (2007). Ionic Liquids in separations. Accounts of Chemical Research, 40(11): 1079-1086. https://doi.org/10.1021/ar700044y

[5] Zhao, H., Xia, S., Ma, P. (2005). Use of Ionic Liquids as 'green' solvents for extractions. Journal of Chemical Technology & Biotechnology: International Research in Process, Environmental & Clean Technology, 80(10): 1089-1096. https://doi.org/10.1002/jctb.1333

[6] Yoshimura, Y., Abe, H., Takekiyo, T., Shigemi, M., Hamaya, N., Wada, R., Kato, M. (2013). Superpressing of a room temperature ionic liquid, 1-ethyl-3-methylimidazolium tetrafluoroborate. The Journal of Physical Chemistry B, 117(40): 12296-12302. https://doi.org/10.1021/jp4055507

[7] Takekiyo, T., Yoshimura, Y. (2020). Peculiar high-pressure phase behavior of 1-butyl-3-methylimidazolium iodide. The Journal of Physical Chemistry B, 124(35): 7659-7667. https://doi.org/10.1021/acs.jpcb.0c04954

[8] Faria, L.F., Ribeiro, M.C. (2015). Phase transitions of triflate-based ionic liquids under high pressure. The Journal of Physical Chemistry B, 119(44): 14315-14322. https://doi.org/10.1021/acs.jpcb.5b08242

[9] Su, L., Li, L., Hu, Y., Yuan, C., Shao, C., Hong, S. (2009). Phase transition of [Cn-mim][PF_6] under high pressure up to 1.0 GPa. The Journal of Chemical Physics, 130(18): 184503. https://doi.org/10.1063/1.3127363

[10] Su, L., Li, M., Zhu, X., Wang, Z., Chen, Z., Li, F., Zhou, Q., Hong, S. (2010). In situ crystallization of low-melting ionic liquid [BMIM][PF_6] under high pressure up to 2 GPa. The Journal of Physical Chemistry B, 114(15): 5061-5065. https://doi.org/10.1021/jp912191z

[11] Su, L., Zhu, X., Wang, Z., Cheng, X., Wang, Y., Yuan, C., Chen, Z., Ma, C., Li, F., Zhou, Q., Cui, Q. (2012). In situ observation of multiple phase transitions in low-

melting ionic liquid [BMIM][BF_4] under high pressure up to 30 GPa. The Journal of Physical Chemistry B, 116(7): 2216-2222. https://doi.org/10.1021/jp2108939

[12] Li, J., Su, L., Zhu, X., Li, H., Cheng, X., Li, L. (2014). Decompression-induced disorder to order phase transition in low-melting ionic liquid [OMIM][PF_6]. Chinese Science Bulletin, 59: 2980-2986. https://doi.org/10.1007/s11434-014-0427-y

[13] Ren, Y., Li, H., Zhu, X., Chen, L., Su, L., Yang, K., Yang, G., Wang, H. (2015). Pressure-induced amorphization of ionic liquid [HMIM][PF_6]. Chemical Physics Letters, 629: 8-12. https://doi.org/10.1016/j.cplett.2015.04.010

[14] Li, H., Su, L., Zhu, X., Cheng, X., Yang, K., Yang, G. (2014). In situ crystallization of ionic liquid [Emim][PF_6] from methanol solution under high pressure. The Journal of Physical Chemistry B, 118(29): 8684-8690. https://doi.org/10.1021/jp500866z

[15] Mao, H.K., Xu, J.A., Bell, P.M. (1986). Calibration of the ruby pressure gauge to 800 kbar under quasi-hydrostatic conditions. Journal of Geophysical Research: Solid Earth, 91(B5): 4673-4676. https://doi.org/10.1029/JB091iB05p04673

[16] Hammersley, A.P., Svensson, S.O., Hanfland, M., Fitch, A.N., Hausermann, D. (1996). Two-dimensional detector software: From real detector to idealised image or two-theta scan. International Journal of High Pressure Research, 14(4-6): 235-248. https://doi.org/10.1080/08957959608201408

[17] Crowder, G.A., Jackson, D. (1971). Infrared and Raman spectra of methyl trifluoroacetate. Spectrochimica Acta Part A: Molecular Spectroscopy, 27(9): 1873-1877. https://doi.org/10.1016/0584-8539(71)80240-4

[18] Crowder, G.A. (1972). Infrared and Raman spectra of vinyl trifluoroacetate. Spectrochimica Acta Part A: Molecular Spectroscopy, 28(8): 1625-1629. https://doi.org/10.1016/0584-8539(72)80133-8

[19] Heimer, N.E., Del Sesto, R.E., Meng, Z., Wilkes, J.S., Carper, W.R. (2006). Vibrational spectra of imidazolium tetrafluoroborate ionic liquids. Journal of Molecular Liquids, 124(1-3): 84-95. https://doi.org/10.1016/j.molliq.2005.08.004

[20] Piermarini, G.J., Block, S., Barnett, J.D. (1973). Hydrostatic limits in liquids and solids to 100 kbar. Journal of Applied Physics, 44(12): 5377-5382. https://doi.org/10.1063/1.1662159

[21] Takemura, K. (2007). Pressure scales and hydrostaticity. High Pressure Research, 27(4): 465-472. https://doi.org/10.1080/08957950701659767

[22] Umebayashi, Y., Fujimori, T., Sukizaki, T., Asada, M., Fujii, K., Kanzaki, R., Ishiguro, S.I. (2005). Evidence of conformational equilibrium of 1-ethyl-3-methylimidazolium in its ionic liquid salts: Raman spectroscopic study and quantum chemical calculations. The Journal of Physical Chemistry A, 109(40): 8976-8982. https://doi.org/10.1021/jp053476j

[23] Li, H., Wang, Z., Chen, L., Wu, J., Huang, H., Yang, K., Wang, Y., Su, L., Yang, G. (2015). Kinetic effect on pressure-induced phase transitions of room temperature ionic liquid, 1-ethyl-3-methylimidazolium trifluoromethanesulfonate. The Journal of Physical Chemistry B, 119(44): 14245-14251. https://doi.org/10.1021/acs.jpcb.5b08384